

Bao Yuan decoction and Tao Hong Si Wu decoction improve lung structural remodeling in a rat model of myocardial infarction: Possible involvement of suppression of inflammation and fibrosis and regulation of the TGF- β 1/Smad3 and NF- κ B pathways

Guozhen Yuan^{1,§}, Anbang Han^{1,§}, Jing Wu¹, Yingdong Lu¹, Dandan Zhang¹, Yuxiu Sun¹, Jian Zhang², Mingjing Zhao³, Bingbing Zhang¹, Xiangning Cui^{1,*}

¹Department of Cardiology, Guang'anmen Hospital, China Academy of Chinese Medical Sciences, Beijing, China;

²Naton Medical Group, Haidian District, Beijing, China;

³The Key Laboratory of Chinese Internal Medicine of the Ministry of Education, Dongzhimen Hospital, Beijing University of Chinese Medicine, Beijing, China.

Summary

Chronic heart failure (CHF) leads to pulmonary structural remodeling, which may be a key factor for poor clinical outcomes in patients with end-stage heart failure, and few effective therapeutic options are presently available. The aim of the current study was to explore the mechanism of action and pulmonary-protective effects of treatment with Bao Yuan decoction combined with Tao Hong Si Wu decoction (BYTH) on lung structural remodeling in rats with ischemic heart failure. In a model of myocardial infarction (MI) induced by ligation of the left anterior descending (LAD) artery, rats were treated with BYTH. Heart function and morphometry were measured followed by echocardiography, histological staining, and immunohistochemical analysis of lung sections. The levels of transforming growth factor- β 1 (TGF- β 1), type I collagen, phosphorylated-Smad3 (p-Smad3), tumor necrosis factor- α (TNF- α), toll-like receptor 4 (TLR4), active nuclear factor κ B (NF- κ B) and alpha smooth muscle actin (α -SMA) were detected using Western blotting. Lung weight increased after an infarct with no evidence of pulmonary edema and returned to normal as a result of BYTH. In addition, BYTH treatment reduced levels of type I collagen, TGF- β 1, and α -SMA expression and decreased the phosphorylation of Smad3 in the lungs of rats after MI. BYTH treatment also reduced the elevated levels of lung inflammatory mediators such as TNF- α , TLR4, and NF- κ B. Results suggested that BYTH could effectively improve lung structural remodeling after MI because of its anti-inflammatory and anti-fibrotic action, which may be mediated by suppression of the TGF- β 1/Smad3 and NF- κ B signaling pathways.

Keywords: Lung remodeling, BYTH, TGF- β 1/Smad3, NF- κ B, myocardial infarction

1. Introduction

Chronic heart failure (CHF) has been singled out as an emerging epidemic, which could be the result of increased incidence and/or increased survival leading to increased prevalence (1). In 60 to 80% of patients, congestive heart failure is complicated by pulmonary

hypertension (PH) (2,3). PH secondary to chronic left ventricular (LV) failure reduces exercise capacity and represents an important independent prognostic factor in sufferers, especially when associated with right ventricular (RV) dysfunction (4,5). However, the lungs are generally neglected by clinicians as therapeutic targets in CHF, except for symptomatic treatment of pulmonary edema. Accordingly, the mechanisms causing PH associated with CHF need to be explored and therapeutic strategies to effectively inhibit that PH need to be devised.

The mechanisms responsible for the pathobiology of PH secondary to chronic LV failure involve both

[§]These authors contributed equally to this work.

*Address correspondence to:

Dr. Xiangning Cui, Department of Cardiology, Guang'anmen Hospital, China Academy of Chinese Medical Sciences, North Line 5, Xicheng District, Beijing 100053, China.
E-mail: cuixiangning@126.com

pulmonary vascular and alveolar septa structural remodeling, which characterized by thickening of the capillary endothelial and alveolar epithelial cell basement membranes with abundant proliferation of myofibroblasts (MFs) and excess deposition of collagen with reticulin (6-9). When CHF develops, the pulmonary alveolar-capillary barrier is subjected to repeated cycles of injury and repair leading to lung parenchymal remodeling, which consists of cellular proliferation and fibrosis leading to the thickening of the inter-alveolar septa (10-12). Lung fibrosis and remodeling are initially adaptive and protect against the development of pulmonary edema, but maladaptive fibrosis and remodeling can have a negative impact on prognosis and contribute to the development of PH. Therefore, novel therapies specifically targeting lung structural remodeling may become available in the future.

Fibrosis and an inflammatory response are typical characteristics of lung structural remodeling following CHF. Transforming growth factor β 1 (TGF- β 1) is a locally generated cytokine that has been implicated as a major contributor to fibroblast proliferation and lung fibrosis. The current authors and other researchers have found that lung TGF- β 1 mRNA and protein levels increase in animal models of heart failure. TGF- β 1 acts by binding to the membrane-bound TGF- β 1 type II receptor (T β RII), which activates T β RI kinase, resulting in the phosphorylation and activation of Smad2/3. Activated Smad2/3 proteins form oligomeric complexes with Smad4 proteins and translocate into the nucleus, where they induce the expression of target genes, including extracellular matrix (ECM) proteins, and thus contribute to the development of lung fibrosis (13,14). The down-regulation of TGF- β expression and modulation of TGF- β /Smad signaling may be effective in preventing lung fibrosis. Animal experiments have also indicated that lung injury associated with CHF is characterized by excessive collagen deposition in the alveoli, inside the vessels, and in the vascular walls of large vessels. This is accompanied by the accumulation of leukocytes and macrophages and increased levels of tumor necrosis factor- α (TNF- α), and Toll-like receptor-4 (TLR4) mRNA or protein in the lungs, suggesting that inflammation also plays an important role in lung structural remodeling (15). Among a variety of transcription regulators, nuclear factor κ B (NF- κ B) has been found to play a critical role in regulating the expression of large numbers of genes encoding inflammatory mediators. In viral induced acute respiratory distress syndrome, treatment with curcumin was found to inhibit the inflammatory response and subsequent pulmonary fibrosis by inhibiting NF- κ B activation and fibroblast differentiation (16). In an animal model of pulmonary fibrosis, administration of NF- κ B pathway inhibitors dramatically inhibited pulmonary fibrogenesis (17-19). Therefore, novel

therapies specifically targeting TGF- β 1 and NF- κ B pathways would be of great potential therapeutic benefit in inhibiting progressive pulmonary remodeling in CHF.

In traditional Chinese medicine, a qi deficiency and blood stasis are the main causes of heart failure. The approach of supplementing qi and increasing blood circulation, or Yiqi Huoxue, is widely used in clinical practice. BaoYuan decoction (BYD) is a typical Chinese medicine to supplement qi and Tao Hong Si Wu decoction (THSWD) is a typical Chinese medicine to increase blood circulation. Both are widely used to treat patients with CHF of any etiology, including coronary heart disease, and chronic obstructive pulmonary disease. BYD was first mentioned in a famous medical text, *Jing Yue Quan Shu*, by Zhang Jingyue in 1624 (during China's Ming Dynasty). THSWD was first described in a well-known medical text, *Yi Zong Jin Jian*, in 1742 (during China's Qing Dynasty). In accordance with Yiqi Huoxue, the traditional Chinese medicines THSWD and BYD were reported to markedly improve heart function in patients with congestive heart failure in conjunction with conventional therapy (20,21). Experimental studies confirmed that THSWD can inhibit proliferation of myocardium interstitial collagenous fibers and expression of collagen protein after acute myocardial infarction (MI) in rats (22), decrease hepatic necroinflammatory disease and fibrosis in an animal model of chronic liver disease (23), and inhibit inflammatory responses by decreasing the expression of TNF- α in cerebral ischemia (24). Both Zhang *et al.* and Du *et al.* found that cardioprotection conferred by BYD was related to attenuation of oxidative stress and inflammatory cell infiltration in CHF post-MI induced by ligation of the left anterior descending (LAD) artery (25,26). In another study, BYD markedly prevented collagen fiber deposition, thus alleviating cardiac fibrosis in cardiac hypertrophy (27). Moreover, the use of BYD (28) in patients with chronic obstructive pulmonary disease had a positive effect on pulmonary function by improving gas diffusion and exercise capacity, suggesting that THSWD and BYD could also have beneficial effects on lung fibrosis and inflammation in CHF. The current study used a post-MI heart failure model to determine whether BYD combined with THSWD (BYTH) improved lung structural remodeling associated with CHF by inhibiting lung inflammation and fibrosis. This study also examined the possible mechanisms for the antifibrotic action of BYTH. The effects of BYTH were compared to those of valsartan. An angiotensin II receptor antagonist commonly used in clinical practice, valsartan is known to protect the heart and lungs during the treatment of CHF (6).

2. Materials and Methods

2.1. Drug preparation

All herbs in BYTH were supplied by traditional

Table 1. Composition of Bao Yuan Tao Hong (BYTH)

Chinese name	Botanical name	Part used	Weight (g)
Ren Shen	<i>Panax ginseng</i> C. A. Meyer	Root	9
Huang Qi	<i>Astragalus membranaceus</i> (Fisch.) Bge.	Root	27
Rou Gui	<i>Cinnamomum cassia</i> Presl.	Bark	4.5
Zhi Gan Cao	<i>Glycyrrhiza uralensis</i> Fisch.	Root and rhizome	9
Shu Di Huang	<i>Rehmannia glutinosa</i> Libosch.	Root tuber	12
Dang Gui	<i>Angelica sinensis</i> (Oliv.) Diels	Root	9
Bai Shao	<i>Paeonia lactiflora</i> Pall.	Root	9
Chuan Xiong	<i>Ligusticum chuanxiong</i> Hort.	Rhizome	6
Tao Ren	<i>Prunus persica</i> (L.) Batsch	Seed	9
Hong Hua	<i>Carthamus tinctorius</i> L.	Flower	9

Chinese medicine pharmacy of Guang'anmen Hospital, China Academy of Chinese Medical Sciences. Species were carefully examined by professional traditional Chinese pharmacists at Guang'anmen Hospital, and the composition and dose are listed in Table 1. The herb mixtures were soaked in 10 volumes (v/w) of distilled water for 90 min and then boiled for 60 min (single decoction of *Panax ginseng*). The decoction was poured into a container. The dregs in the original container were added to 8 volumes (v/w) of distilled water and boiled again for 60 min. The two decoctions were mixed together and filtered repeatedly through a 100-mesh sieve to yield a concentration of 1 g of crude drug/mL. The pre-prepared decoction was poured in a centrifuge tube and stored at 4°C before use. BYTH was administered by oral gavage at a dose of 15 g/kg/day in this study. Valsartan (batch number X1428), manufactured by Beijing Novartis Pharmaceutical Co. Ltd., was dissolved in sterile water.

2.2. Animal model and administration

Male Sprague-Dawley (SD) rats (220-250 g) were donated by Beijing Vital River Laboratory Animal Technology Co. Ltd. (animal license number: SCXK (Beijing) 2012-0001). All animal experimental procedures and protocols were approved by the Institutional Animal Care and Use Committee of Guang'anmen Hospital, China Academy of Chinese Medical Sciences. A rat model of CHF was created by inducing MI following ligation of the LAD artery (25,26,29-32). Briefly, rats were intra-peritoneally anaesthetized with 1% sodium pentobarbital solution (50 mg/kg), intubated, and placed on a rodent ventilator (Huaihe Apparatus, Shanghai). A left-sided thoracotomy was performed in order to expose the heart, and the proximal left anterior descending coronary artery was ligated. The sham group underwent the same procedure with the exception of ligation of the artery. A 12-lead ECG was recorded before and after surgery. Rats after MI were fed normally for 4 weeks. Based on the results of transthoracic echocardiography (Table 2), the surviving rats were randomly assigned to the following groups: a CHF group ($n = 12$), a sham group ($n = 10$), a BYTH

Table 2. Echocardiographic ejection fraction levels in the study groups before treatment with BYTH ($x \pm s$)

Group	n	EF (%)
Sham	10	84.490 ± 7.3354
CHF	12	44.708 ± 8.4369*
BYTH	10	46.863 ± 9.0312*
Valsartan	9	47.911 ± 9.1068*

*: $p > 0.05$ vs. the sham group

group ($n = 10$), and a valsartan group ($n = 9$). BYTH (15 g/kg) and valsartan (10 mg/kg) were administered by gavage once a day for 4 weeks. An equal volume of distilled water was administered to the CHF and sham groups.

2.3. Transthoracic echocardiography

Rats in each group were examined to evaluate the morphology and function of the left ventricle using noninvasive transthoracic echocardiography. Short-axis images were obtained at the papillary muscle level and 2-D-guided M-mode tracings were recorded at a speed of 200 mm/s. Anterior and posterior end-diastolic wall thickness and LV internal dimensions were measured and the percent fractional shortening (FS%) was calculated. Left atrial (LA) volume, LV end-diastolic volume (EDV), LV end-systolic volume (ESV), LV ejection fraction (EF), LV end-diastolic dimension (LVIDd), and LV end-systolic dimension (LVIDs) were measured and calculated from apical views.

2.4. Sample preparation

At the end of 4 weeks, the rats were sacrificed by removing the heart, lung, and other major organs under abundant anesthesia, and the organs were immediately weighed. Lung tissue was dried at 58°C to a constant weight. The relative water content in lung tissue was calculated. The left lung and left ventricle were snap frozen in liquid nitrogen pending biochemical analysis. The airway of the upper right lobe and the heart were subsequently fixed in 4% paraformaldehyde and embedded in paraffin for histological analysis.

2.5. Hematoxylin and eosin (HE) and Masson staining

Rat lungs and hearts were fixed in formalin for 48 h, embedded in paraffin, and sectioned into 4-mm thick slices for HE staining or Masson staining. After slides with stained tissue slices were sealed with neutral gum, they were microscopically examined at the appropriate magnification. Color images of five randomly chosen microscopic fields were obtained from each slice. Medical imaging software (NIH image, Bethesda, MD) was used to semi-quantitatively determine the area density (AD) *i.e.* the area of collagen fibers with respect to the area of the lung.

2.6. Immunohistochemical staining

Immunohistochemical staining for smooth muscle α -actin (α -SMA) was used to identify smooth muscle cells or myofibroblasts (using a mouse monoclonal anti- α smooth muscle actin antibody, Abcam, Inc.), and staining for NF- κ B was performed on 4- μ m sections of tissue deparaffinized using xylene. Endogenous peroxidase was quenched with 3% H₂O₂ for 10 min. The antigen was recovered in Tris-EDTA buffer (pH = 9.0) for 2 min and 30 s at 140°C and then washed in phosphate-buffered saline (PBS). The sections were incubated with monoclonal anti α -SMA antibody (1:200, Abcam, Inc.) or rabbit anti-NF- κ B p65 (1:200; Santa Cruz, Inc.) at 37°C for 1 h followed by biotinylated secondary antibody for 20 min. The sections were stained with diaminobenzidine chromogen and counterstained with hematoxylin.

2.7. Western blot analysis

Total protein was obtained from heart and lung tissues by sonication, centrifugation, and heat denaturation. The protein lysates were electrophoresed and separated on 10% sodium dodecyl sulfate-polyacrylamide gels and then transferred onto nitrocellulose membranes (Millipore, Inc, USA). The membranes were blocked with 5% skim milk at room temperature for 1 h and then incubated overnight at 4°C with primary antibodies, including rabbit polyclonal Anti-Collagen I (1:800, Abcam, Inc.), mouse monoclonal anti-TGF- β 1 (1:500, Abcam, Inc.), rabbit monoclonal anti-Smad3 (phosphor C25A9) (1:500, Cell Signaling Technology, Inc.), rabbit polyclonal anti-TNF- α (1:1000, Abcam, Inc.), mouse monoclonal anti-TLR4 (1:2000, Abcam, Inc.), and rabbit anti-NF- κ B p65 (1:800; Santa Cruz, Inc.). The membranes were then incubated with the secondary antibody (1:2000) at room temperature for 2 h. Electrochemiluminescence was induced and the Gene Gnome Gel Imaging System (Syngene Co.) was used to capture the resulting images. Image J (NIH image, Bethesda, MD) was used to analyze the gel images. The results were expressed as density values normalized to GAPDH.

2.8. Statistical analysis

Data were expressed as the mean \pm standard deviation. The statistical significance of differences between mean values was determined using one-way analysis of variance (ANOVA), and a *p* value of less than 0.05 was considered significant. Statistical calculations were performed using the software SPSS version 19.0.

3. Results

3.1. Effects of BYTH on LV function and LV remodeling

LV echocardiographic parameters are shown in Figure 1. The ejection fraction and fractional shortening measurements were greater in the BYTH group and the valsartan group than those in the CHF group (*p* < 0.05) (Figure 1B and 1C), while the end-systolic volume and LV end-systolic dimension measurements were smaller (*p* < 0.05) (Figure 1D and 1E). Although the EDV and LVIDd tended to decrease in both the BYTH and the valsartan groups versus those in the CHF group, the difference was not statistically significant (*p* > 0.05) (Figure 1F and 1G). EF and FS measurements in the CHF group, the BYTH group, and the valsartan group were smaller than those in the sham group (*p* < 0.05) (Figure 1B and 1C), while the ESV and LVIDs increased (*p* < 0.05) (Figure 1D and 1E). Histological study revealed that the fractional area of collagen in the LV (Figure 2A and 2B) increased markedly in the CHF group in comparison to that in the sham group (*p* < 0.05), and that area decreased as a result of BYTH and valsartan treatment. The parameters of LV remodeling and dysfunction were significantly altered by BYTH treatment.

3.2. Effects of BYTH on pulmonary structural remodeling

As shown in Figure 3, the wet lung/body weight ratio increased after MI (*p* < 0.05) and BYTH and valsartan markedly improved this ratio (*p* < 0.05) (Figure 3A). Similarly, the dry lung/body weight ratio increased after MI (*p* < 0.05), providing evidence of substantial pulmonary remodeling; treatment with BYTH and valsartan reversed the increase in this ratio (*p* < 0.05) (Figure 3B). The dry/wet lung weight ratio was comparable among all groups, suggesting that no significant edema occurred (Figure 3C).

HE staining revealed intact and clear alveoli, normal interstitium, and few inflammatory cells in the lungs of the sham group. However, the CHF group had LV dysfunction caused by progressive lung injury, as evinced by destruction of lung alveoli, inflammatory cell infiltration, and thickening of the lung interstitium. BYTH or valsartan treatment prevented these changes in the lungs of rats after MI. Interestingly, the CHF group had prominent pulmonary vascular and perivascular

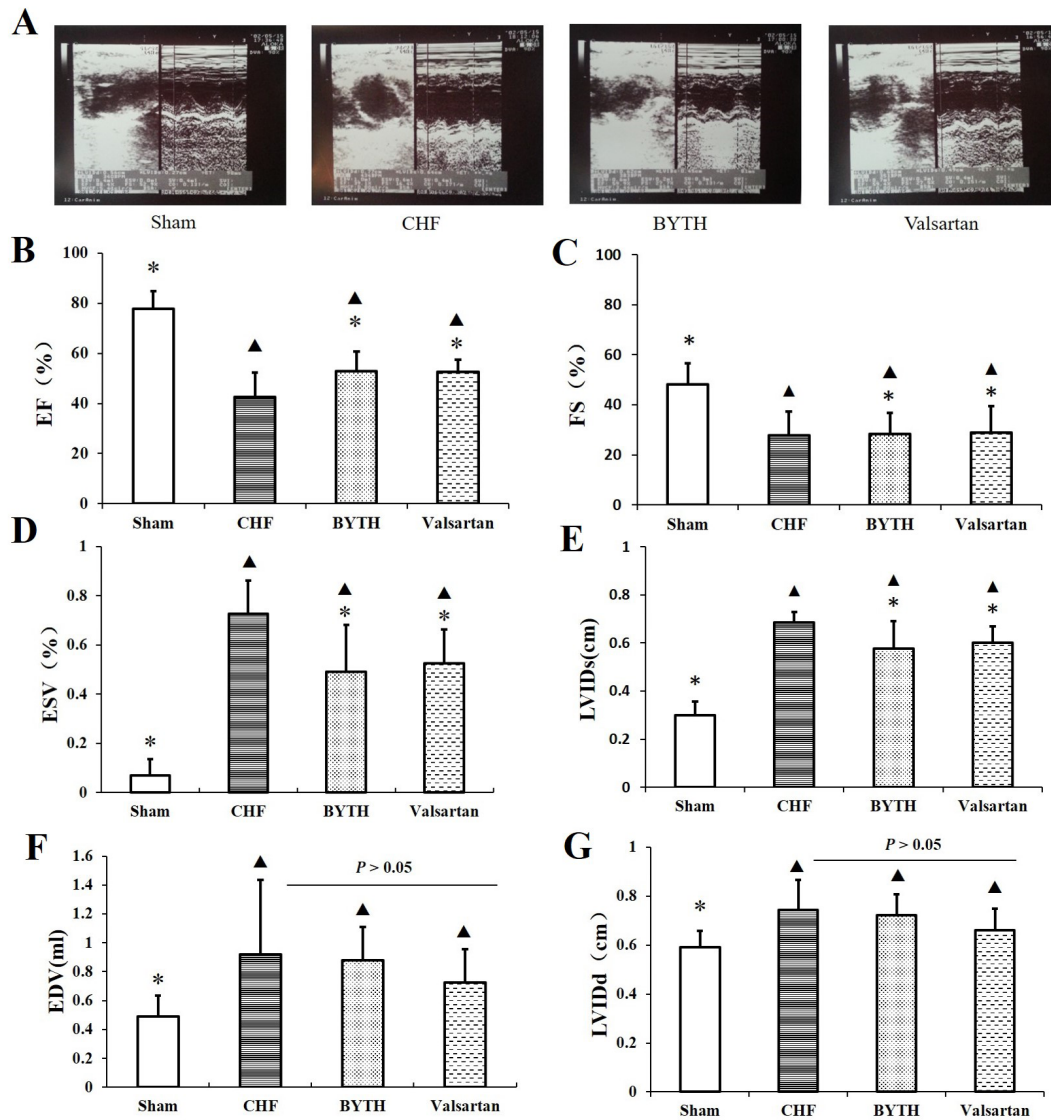


Figure 1. Effects of BYTH on echocardiographic left ventricular (LV) function in rats with CHF. (A) Typical echocardiography images; (B) LV ejection fraction (EF); (C) LV fractional shortening (FS); (D) LV end-systolic volume (ESV); (E) LV end-systolic dimensions (LVIDs); (F) LV end-diastolic volume (EDV) and (G) LV end-diastolic dimension (LVIDd) (▲ $p < 0.05$ vs. the sham group, * $p < 0.05$ vs. the CHF group).

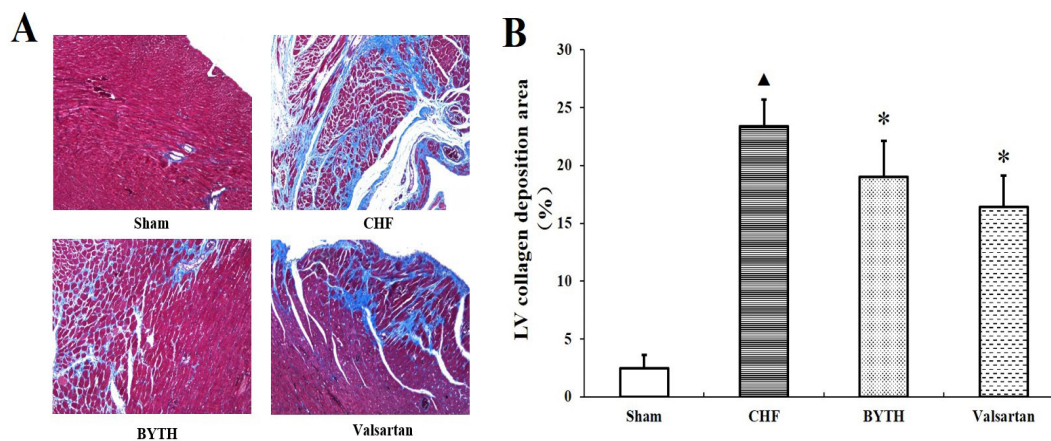


Figure 2. Effects of BYTH on myocardial fibrosis in rats with CHF. (A) Representative Masson Trichrome-stained LV areas are shown and blue areas indicate fibrotic staining ($\times 10$); (B) Fibrosis was measured in the whole LV section, and 5 sections were calculated for each heart (▲ $p < 0.05$ vs. the sham group, * $p < 0.05$ vs. the CHF group).

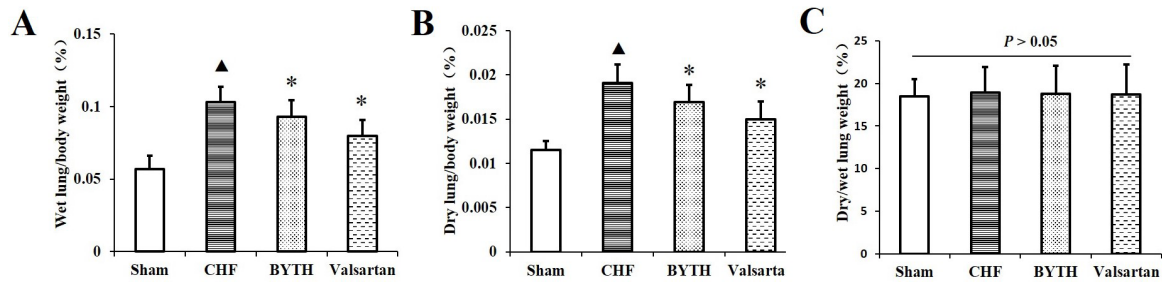


Figure 3. Effect of BYTH on lung weight in rats with CHF. (A) Wet lung/body weight; (B) Dry lung/body weight; (C) Ratio of dry/wet lung weight. (▲ $p < 0.05$ vs. the sham group, * $p < 0.05$ vs. the CHF group).

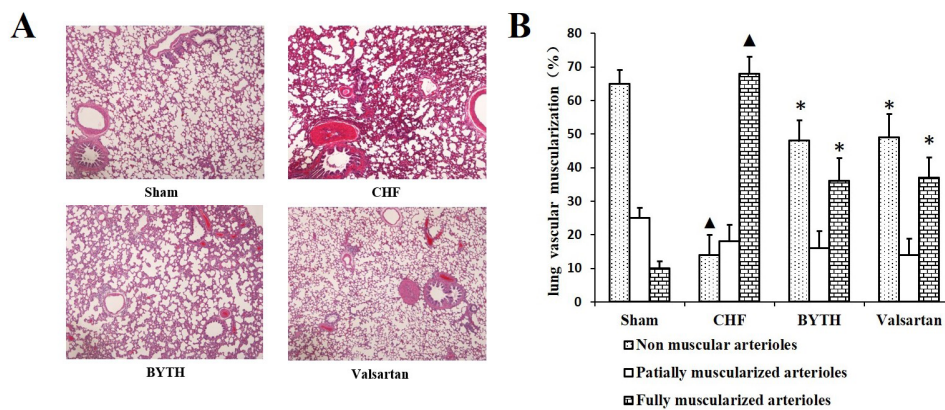


Figure 4. Effects of BYTH on lung vascular masculinization in rats with CHF. (A) Histological lung section with hematoxylin and eosin staining ($\times 40$); (B) Quantitative analysis of the distribution of non-muscular, partially muscular, and fully muscularized small arteries (▲ $p < 0.05$ vs. the sham group, * $p < 0.05$ vs. the CHF group).

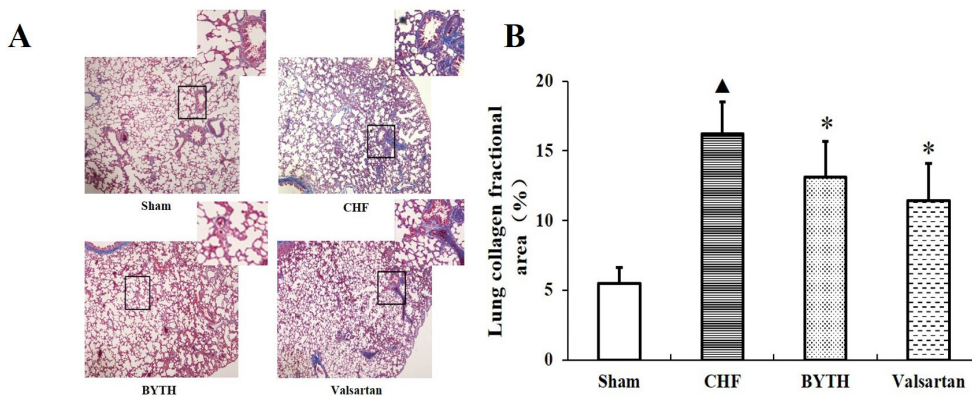


Figure 5. Effects of BYTH on pulmonary structural remodeling in rats with CHF. (A) Masson's trichrome staining for collagen in blue ($\times 40$); (B) Quantitative analysis of lung collagen deposition (▲ $p < 0.05$ vs. the sham group, * $p < 0.05$ vs. the CHF group).

remodeling. LV dysfunction also caused an increase in fully muscularized (FM) small arteries, but there were significantly fewer FM small arteries in rats in the BYTH and valsartan groups compared to the number in the CHF group. Similarly, the BYTH treatment group had significantly more non-muscularized (NM) small arteries compared to the CHF group (Figure 4), indicating that BYTH and valsartan significantly improved lung vascular remodeling induced by ligation

of the LAD artery. Masson trichrome staining also revealed intact alveoli and normal interstitium in the lungs of rats in the sham group. Ligation of the LAD artery resulted in greater destruction of lung alveoli, thickening of interstitium, and fibroblast diffusion in rat lungs, and BYTH or valsartan treatment significantly halted these changes in rat lungs after MI (Figure 5). α -SMA expression has been extensively used as a marker of fibroblast differentiation into its activated state, the

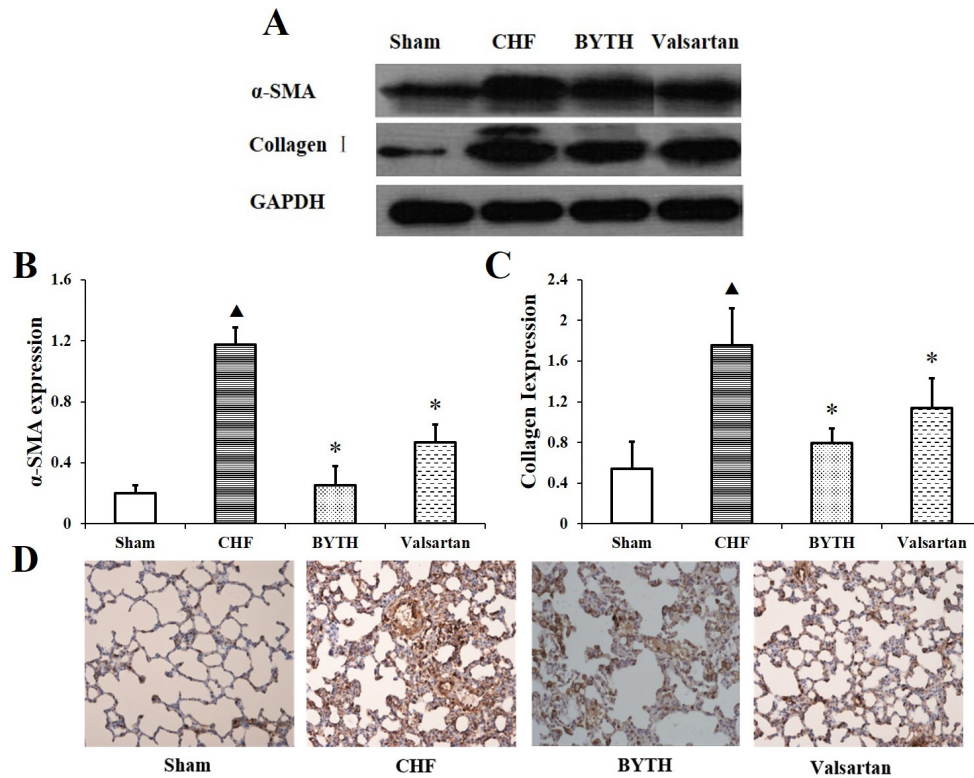


Figure 6. Effects of BYTH on expression of proteins related to lung fibrosis in rats with CHF. (A) and (B) Expression of α -SMA; (A) and (C) Expression of type I collagen; (D) Immunohistochemistry for α -SMA; original magnification $\times 100$ ($\blacktriangle p < 0.05$ vs. the sham group, $*p < 0.05$ vs. the CHF group).

myofibroblast. Expression of α -SMA increased in the interalveolar septa of animals after MI compared to its expression in the sham group; however, BYTH and valsartan treatment significantly reduced that expression (Figure 6).

α -SMA-positive MFs actively synthesize ECM components. Type I collagen, the main collagen isoform produced by fibroblasts in many fibrotic processes, was measured in the current study. Western blotting revealed that type I collagen deposition was significantly greater in rats in the CHF group compared to that in the sham group; however, BYTH significantly decreased the expression of type I collagen protein in the lungs (Figure 6). Together, these findings indicate that the parameters of lung tissue fibrotic remodeling were significantly reversed by BYTH and valsartan treatment.

3.3. Effects of BYTH on the TGF- β 1/Smad3 signaling pathway in rat lungs after CHF

CHF markedly increased the level of TGF- β 1 protein in treated rat compared to that in the sham group at the endpoint of 4 weeks; however, BYTH and valsartan treatment significantly reduced the level of TGF- β 1 expression compared to that in the CHF group (Figure 7). Similarly, CHF markedly increased the level of p-Smad3 protein in the lungs of treated rats compared to that in the sham group, and BYTH and valsartan treatment

significantly reduced p-Smad3 expression compared to that in the CHF group (Figure 7).

3.4. Effects of BYTH on the NF- κ B signaling pathway in rat lungs after CHF

As shown in Figure 8, results indicated that the CHF group had increased expression of lung TNF- α , TLR4, and NF- κ B p65 protein compared to expression in the sham group. After 4 weeks of treatment, BYTH significantly reversed those changes (Figure 8).

4. Discussion

The current results indicated that treatment with BYTH protects the pulmonary structure and cardiac function in rats after MI. After MI, rats developed CHF with major lung structural remodeling characterized by alveolar wall collagen deposition, a dramatic increase in the percentage of FM lung vessels, and an increase in expression of inflammatory cytokines in lung tissues. Treatment with BYTH and valsartan reduced lung and vascular fibrosis, fibroblast proliferation, and proinflammatory cytokine expression. The mechanism for this action may involve suppression of TGF- β 1/Smad3 and NF- κ B signaling. The current results suggest that BYTH has some direct beneficial effects on pulmonary fibrosis and the inflammatory response following CHF.

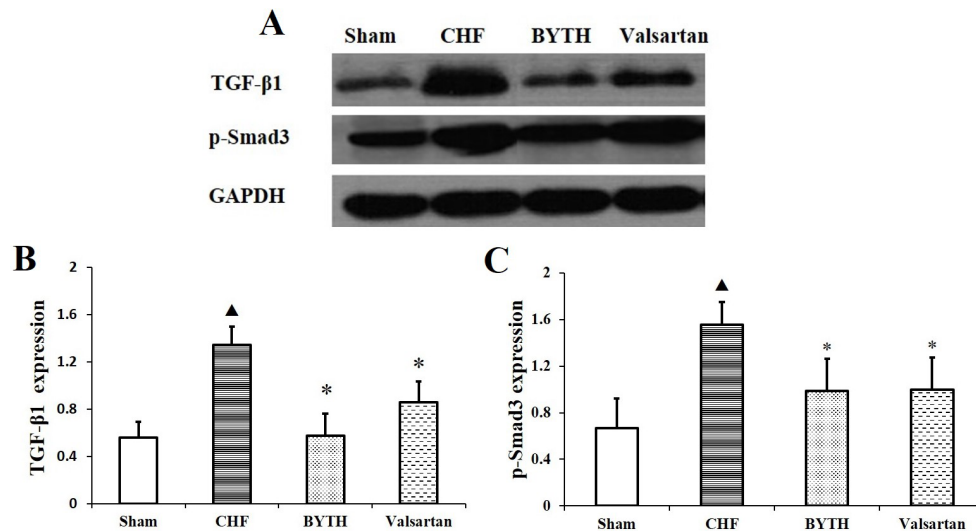


Figure 7. Effects of BYTH on lung TGF- β 1/Smad3 signaling pathway expression in rats with CHF. (A) and (B) Expression of transforming growth factor TGF- β 1; (A) and (C) Expression of p-Smad3 ($\blacktriangle p < 0.05$ vs. the sham group, $*p < 0.05$ vs. the CHF group).

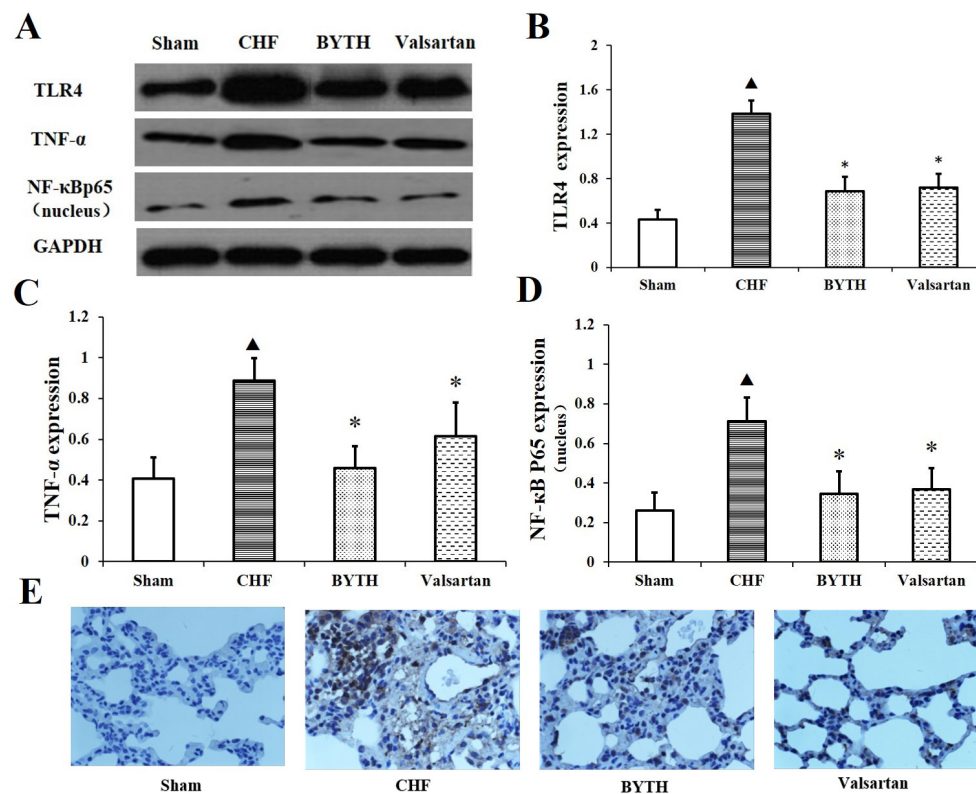


Figure 8. Effects of BYTH on expression of protein related to lung inflammation in rats with CHF. (A) and (B) Expression of TLR4; (A) and (C) Expression of TNF- α ; (A) and (D) The activation of NF- κ B; (E) Immunohistochemistry for NF- κ B; Original magnification $\times 100$ ($\blacktriangle p < 0.05$ vs. the sham group, $*p < 0.05$ vs. the CHF group).

The lungs are the organs most affected by CHF. In patients with CHF, an elevation in the LV filling pressure results in a passive increase in pulmonary venous pressure and pulmonary alveolar-capillary stress failure, resulting in cycles of alveolar wall injury and repair. Consequently, pathological morphological changes occur in small pulmonary arteries as well as in the alveolar-

epithelial units and the ECM (8,33-36). This reparative "scarring" process causes a restrictive lung syndrome characterized by impaired gas exchange (37), a reduction in lung volume, and decreased lung compliance. This pathological process may also contribute to type 2 PH (PH secondary to chronic LV failure), further increase the RV afterload and RV dysfunction, and ultimately

cause heart failure. Lung structural remodeling may be a key factor for poor clinical outcomes in patients with end-stage heart failure. Thus, the effective treatment of LV end-stage heart failure may require additional action to reduce lung fibrosis.

The current results revealed that the total lung weight in the CHF group increased while water content in the lungs decreased. This indicates that, in CHF models, the pulmonary weight increase is due to structural remodeling with abundant proliferation of MFs and excess collagen, elastin, and reticulin deposition (ECM deposition) rather than edema. MFs have been found to play a key role in animal as well as human pulmonary fibrotic disorders (38). MFs are characterized by the expression of α -SMA, as well as excessive production of collagenous ECM after tissue injury. The current study found that excessive collagen deposition and upregulated α -SMA protein expression in lungs after MI were both reversed by BYTH treatment, suggesting that BYTH may have anti-fibrotic action by inhibiting MF proliferation and collagen production.

From the perspective of traditional Chinese medicine, the fundamental problem in heart failure post-MI is the prolonged deficiency of qi in the heart, which causes the heart to become too weak to move blood and transport fluid, leading to blood "stasis" and phlegm "stagnation," resulting in accumulation in the heart and lungs. These concepts are consistent with the pathological changes of collagen deposition and interstitial fibrosis. The heart and lungs are closely related, and the approach of supplementing qi and increasing blood circulation, or Yiqi Huoxue, is widely used in the treatment of cardiac and pulmonary diseases. BYD is a typical Chinese medicine to supplement qi and THSWD is a typical Chinese medicine to increase blood circulation. BYTH consists of BYD and THSWD, which include 10 Chinese herbs. The main active ingredients of those medicines are *Astragalus membranaceus* and *Panax ginseng*, which invigorate qi in the heart and lungs. Peach pits, *Carthamus tinctorius*, *Ligusticum chuanxiong*, and *Radix angelicae sinensis* increase blood circulation and eliminate the stasis of blood, water, and phlegm. Modern pharmacological research has indicated that ginseng, one of the main components of BYTH, has cardiovascular benefits and is therefore usually used to treat heart disease (39). Emerging evidence also suggests that ginseng attenuates myocardial hypertrophy, thus blunting the processes of remodeling and heart failure (40). *Astragalus* injections can enhance myocardial contractility, improve circulation, protect myocardial cells, and regulate immunity (41). The current study found that BYTH protects from cardiac and pulmonary injury induced by MI in rats.

TGF- β 1 is a locally generated cytokine that has been implicated as a major contributor to fibroblast proliferation and tissue fibrosis in various organ systems. Increased lung TGF- β 1 mRNA and protein levels

in mice with heart failure suggest that the TGF- β 1 signaling pathway might contribute to the development of lung fibrosis and remodeling in this model (42). As a main downstream signal transducer of TGF- β 1, Smad3 can be phosphorylated by an activated type I receptor of TGF- β 1. It then forms a complex with Smad4 and translocates into the nucleus, where it acts as a transcription factor and it promotes the expression of target genes including type I and type III collagen. The current study indicated that lung TGF- β 1 protein expression increased in rats with heart failure following MI, and the level of p-Smad3 also increased markedly; both were reversed by BYTH. These results suggest that the significant activation of the TGF- β 1/Smad3 signaling pathway in lung tissues after CHF can lead to fibroblast proliferation and a marked upregulation of type I collagen expression. BYTH may disrupt the TGF- β 1/Smad3 signaling pathway, which may be why it attenuates lung fibrosis in CHF.

Inflammation is an integral part of the healing response to lung injury induced by CHF. While inflammation may be beneficial in the short term (for example, by inducing immune responses that lead to the eradication of pathogens), chronic inflammation and the associated regenerative wound healing response are closely linked to the development of fibrosis. In the inflammatory cascade, NF- κ B is a predominant regulator of inflammatory cytokines. Activated NF- κ B increases the expression of TGF- β 1, TNF- α , and IL-1 β , which subsequently activate collagen deposition and fibrosis that lead to lung structural remodeling. Inhibition of the NF- κ B pathway can ameliorate pulmonary inflammation and fibrosis. Thus, NF- κ B signaling plays an important role in both fibrosis and an inflammatory response. An inflammatory response is usually associated with the activation of innate immunity. Recent studies have suggested that lung TLR4 expression both at the mRNA and protein level increased in mice with heart failure (15). TLR4-mediated pathways played a key role in triggering the lung inflammatory response by activating the NF- κ B system. The current study revealed increased expression of lung TLR4, NF- κ B, and TNF- α following the induction of MI, and treatment with BYTH significantly decreased the expression of those inflammatory markers. The pulmonary protective effects of BYTH may be because it suppresses the TLR4/NF- κ B signaling pathway.

In conclusion, the current study revealed that treatment with BYTH has notable benefits in terms of preventing lung structural remodeling following MI. The potential mechanisms of that action may be associated with the anti-fibrotic and anti-inflammatory action of BYTH on lung issue. Based on the current results, BYTH has anti-fibrotic action mainly by suppressing the TGF- β 1/Smad3 signaling pathway, which might contribute to its attenuation of myofibroblast proliferation and collagen deposition. The possible mechanisms may

also involve inhibition of the excessive expression of the TLR4-NF- κ B pathway.

Acknowledgements

This work was supported by a grant from the National Natural Science Foundation of China (Grant No. 81273945).

References

1. Roger VL. The heart failure epidemic. *Int J Environ Res Public Health*. 2010; 7:1807-1830.
2. Ghio S, Gavazzi A, Campana C, Inserra C, Klersy C, Sebastiani R, Arbustini E, Recusani F, Tavazzi L. Independent and additive prognostic value of right ventricular systolic function and pulmonary artery pressure in patients with chronic heart failure. *J Am Coll Cardiol*. 2001; 37:183-188.
3. Lam CS, Roger VL, Rodeheffer RJ, Borlaug BA, Enders FT, Redfield MM. Pulmonary hypertension in heart failure with preserved ejection fraction: A community-based study. *J Am Coll Cardiol*. 2009; 53:1119-1126.
4. Abramson SV, Burke JF, Kelly JJ, Kitchen JG, Dougherty MJ, Yih DF, McGeehin FC, Shuck JW, Phiambolis TP. Pulmonary hypertension predicts mortality and morbidity in patients with dilated cardiomyopathy. *Ann Intern Med*. 1992; 116:888-895.
5. Butler J, Chomsky DB, Wilson JR. Pulmonary hypertension and exercise intolerance in patients with heart failure. *J Am Coll Cardiol*. 1999; 34:1802-1806.
6. Huang W, Kingsbury MP, Turner MA, Donnelly JL, Flores NA, Sheridan DJ. Capillary filtration is reduced in lungs adapted to chronic heart failure: morphological and haemodynamic correlates. *Cardiovasc Res*. 2001; 49:207-217.
7. Jasmin JF, Calderone A, Leung TK, Villeneuve L, Dupuis J. Lung structural remodeling and pulmonary hypertension after myocardial infarction: Complete reversal with irbesartan. *Cardiovasc Res*. 2003; 58:621-631.
8. Kingsbury MP, Huang W, Donnelly JL, Jackson E, Needham E, Turner MA, Sheridan DJ. Structural remodelling of lungs in chronic heart failure. *Basic Res Cardiol*. 2003; 98:295-303.
9. Gehlbach BK, Geppert E. The pulmonary manifestations of left heart failure. *Chest*. 2004; 125:669-682.
10. West JB, Mathieu-Costello O. Vulnerability of pulmonary capillaries in heart disease. *Circulation*. 1995; 92:622-631.
11. Townsley MI, Fu Z, Mathieu-Costello O, West JB. Pulmonary microvascular permeability. Responses to high vascular pressure after induction of pacing-induced heart failure in dogs. *Circ Res*. 1995; 77:317-325.
12. Guazzi M. Alveolar-capillary membrane dysfunction in heart failure: Evidence of a pathophysiologic role. *Chest*. 2003; 124:1090-1102.
13. Mackinnon AC, Gibbons MA, Farnworth SL, Leffler H, Nilsson UJ, Delaine T, Simpson AJ, Forbes SJ, Hirani N, Gaudie J. Regulation of transforming growth factor- β 1-driven lung fibrosis by galectin-3. *Am J Respir Crit Care Med*. 2012; 185:537-546.
14. Chen T, Nie H, Gao X, Yang J, Pu J, Chen Z, Cui X, Wang Y, Wang H, Jia G. Epithelial-mesenchymal transition involved in pulmonary fibrosis induced by multi-walled carbon nanotubes *via* TGF- β /Smad signaling pathway. *Toxicol Lett*. 2014; 226:150-162.
15. Chen Y, Guo H, Xu D, Xu X, Wang H, Hu X, Lu Z, Kwak D, Xu Y, Gunther R, Huo Y, Weir EK. Left ventricular failure produces profound lung remodeling and pulmonary hypertension in mice heart failure causes severe lung disease. *Hypertension*. 2012; 59:1170-1178.
16. Avasarala S, Zhang F, Liu G, Wang R, London SD, London L. Curcumin modulates the inflammatory response and inhibits subsequent fibrosis in a mouse model of viral-induced acute respiratory distress syndrome. *PLoS One*. 2012; 8:e57285.
17. Cao H, Zhou X, Zhang J, Huang X, Zhai Y, Zhang X, Chu L. Hydrogen sulfide protects against bleomycin-induced pulmonary fibrosis in rats by inhibiting NF- κ B expression and regulating Th1/Th2 balance. *Toxicol Lett*. 2013; 224:387-394.
18. Chitra P, Saiprasad G, Manikandan R, Sudhandiran G. Berberine attenuates bleomycin induced pulmonary toxicity and fibrosis *via* suppressing NF- κ B dependant TGF- β activation: A biphasic experimental study. *Toxicol Lett*. 2013; 219: 178-193.
19. El-Khouly D, El-Bakly WM, Awad AS, El-Mesallamy HO, El-Demerdash E. Thymoquinone blocks lung injury and fibrosis by attenuating bleomycin-induced oxidative stress and activation of nuclear factor Kappa-B in rats. *Toxicology*. 2012; 302:106-113.
20. Li DP, Chen Q, Yi L. Effects of yiqi huoxue method on cardiac function in patients with congestive heart failure. *Zhongguo Zhong Xi Yi Jie He Za Zhi*. 2006; 26:552-554. (in Chinese)
21. Sun CC, Gao SS. Clinical observation on treating heart failure with Baoyuan decoction and Taohong Siwu decoction. *Clinical Journal of Chinese Medicine*. 2014; 6:62-63. (in Chinese)
22. Zhou YC, Liu B, Wang J, Sun XG, Huang GQ, Zeng YJ, Chen J. Influence of Taohong Siwu decoction on myocardium interstitial collagen reconstitution after acute myocardial infarction in rats. *Chinese Journal of Experimental Traditional Medical Formulae*. 2011; 17:152-155. (in Chinese)
23. Xi S, Shi M, Jiang X, Minuk GY, Cheng Y, Peng Y, Gong Y, Xu Y, Wang X, Yang J, Yue L, Wang Y. The effects of Tao-Hong-Si-Wu on hepatic necroinflammatory activity and fibrosis in a murine model of chronic liver disease. *J Ethnopharmacol*. 2016; 180:28-36.
24. Yen TL, Ong ET, Lin KH, Chang CC, Jayakumar T, Lin SC, Fong TH, Sheu JR. Potential advantages of Chinese medicine Taohong Siwu Decoction () combined with tissue-plasminogen activator for alleviating middle cerebral artery occlusion-induced embolic stroke in rats. *Chin J Integr Med*. 2014:1-9.
25. Zhang Y, Li C, Meng H, Guo D, Zhang Q, Lu W, Wang Q, Wang Y, Tu P. BYD ameliorates oxidative stress-induced myocardial apoptosis in heart failure post-acute myocardial infarction *via* the P38 MAPK-CRYAB signaling pathway. *Front Physiol*. 2018; 9:505.
26. Du Z, Shu Z, Lei W, Li C, Zeng K, Guo X, Zhao M, Tu P, Jiang Y. Integration of metabolomics and transcriptomics reveals the therapeutic effects and mechanisms of Baoyuan decoction for myocardial ischemia. *Front Pharmacol*. 2018; 9:514.
27. Du Z, Wen R, Liu Q, Wang J, Lu Y, Zhao M, Guo X,

- Tu P, Jiang Y. 1H NMR-based dynamic metabolomics delineates the therapeutic effects of Baoyuan decoction on isoproterenol-induced cardiac hypertrophy. *J Pharm Biomed Anal.* 2018; 163:64-77.
28. Wu CJ, Xie XM. Thirty cases with chronic obstructive pulmonary disease at acute and aggravated stage treated with Original Qi Preserving decoction. *Henan Traditional Chinese Medicine.* 2015; 35:2167-2168. (in Chinese)
 29. Samsamshariat SA, Samsamshariat ZA, Movahed MR. A novel method for safe and accurate left anterior descending coronary artery ligation for research in rats. *Cardiovasc Revasc Med.* 2005; 6:121-123.
 30. Muthuramu I, Lox M, Jacobs F, De Geest B. Permanent ligation of the left anterior descending coronary artery in mice: A model of post-myocardial infarction remodelling and heart failure. *J Vis Exp.* 2014; 2: e52206.
 31. Liang T, Zhang Y, Yin S, Gan T, An T, Zhang R, Wang Y, Huang Y, Zhou Q, Zhang J. Cardio-protecteffect of qiliqiangxin capsule on left ventricular remodeling, dysfunction and apoptosis in heart failure rats after chronic myocardial infarction. *Am J Transl Res.* 2016; 8:2047-2058.
 32. Luo J, Chen X, Luo C, Lu G, Peng L, Gao X, Zuo Z. Hydrochlorothiazide modulates ischemic heart failure-induced cardiac remodeling *via* inhibiting angiotensin II type 1 receptor pathway in rats. *Cardiovasc Ther.* 2017; 35: e12246.
 33. Delgado JF, Conde E, Sánchez V, López-Ríos F, Gómez-Sánchez MA, Escribano P, Sotelo T, Gómez de la Cámara A, Cortina J, de la Calzada CS. Pulmonary vascular remodeling in pulmonary hypertension due to chronic heart failure. *Eur J Heart Fail.* 2005; 7:1011-1016.
 34. Townsley M, Snell KS, Ivey CL, Culberson DE, Liu DC, Reed RK, Mathieu-Costello O. Remodeling of lung interstitium but not resistance vessels in canine pacing-induced heart failure. *J Appl Physiol (1985).* 1999; 87:1823-1830.
 35. Ahmed MS, Øie E, Vinge LE, von Lueder TG, Attramadal T, Attramadal H. Induction of pulmonary connective tissue growth factor in heart failure is associated with pulmonary parenchymal and vascular remodeling. *Cardiovasc Res.* 2007; 74:323-333.
 36. Jiang BH, Tardif JC, Sauvageau S, Ducharme A, Shi Y, Martin JG, Dupuis J. Beneficial effects of atorvastatin on lung structural remodeling and function in ischemic heart failure. *J Card Fail.* 2010; 16:679-688.
 37. Cahalin LP, Chase P, Arena R, Myers J, Bensimhon D, Peberdy MA, Ashley E, West E, Forman DE, Pinkstaff S, Lavie CJ, Guazzi M. A meta-analysis of the prognostic significance of cardiopulmonary exercise testing in patients with heart failure. *Heart Fail Rev.* 2013; 18:79-94.
 38. Zhang K, Rekhter MD, Gordon D, Phan SH. Myofibroblasts and their role in lung collagen gene expression during pulmonary fibrosis. A combined immunohistochemical and in situ hybridization study. *Am Journal Pathol.* 1994; 145:114-125.
 39. Zheng SD, Wu HJ, Wu DL. Roles and mechanisms of ginseng in protecting heart. *Chin J Integr Med.* 2012; 18:548-555.
 40. Karmazyn M, Moey M, Gan XT. Therapeutic potential of ginseng in the management of cardiovascular disorders. *Drugs.* 2011; 71:1989-2008.
 41. Zhang JG, Gao DS, Wei GH. Clinical study on effect of Astragalus injection on left ventricular remodeling and left ventricular function in patients with acute myocardial infarction. *Zhongguo Zhong Xi Yi Jie He Za Zhi.* 2002; 22:346-348. (in Chinese)
 42. Ikeuchi M, Tsutsui H, Shiomi T, Matsusaka H, Matsushima S, Wen J, Kubota T, Takeshita A. Inhibition of TGF-beta signaling exacerbates early cardiac dysfunction but prevents late remodeling after infarction. *Cardiovasc Res.* 2004; 64:526-535.

(Received October 8, 2018; Revised October 27, 2018; Accepted October 29, 2018)